Analytical Methods

ROYAL SOCIETY OF CHEMISTRY

PAPER

View Article Online
View Journal | View Issue



Cite this: *Anal. Methods*, 2020, **12**, 5885

# A wearable fluidic collection patch and ion chromatography method for sweat electrolyte monitoring during exercise†

Annemarijn S. M. Steijlen, *[a] Jeroen Bastemeijer,[a] Pim Groen,[b] Kaspar M. B. Jansen,[c] Patrick J. French[a] and Andre Bossche[a]

Received 30th October 2020
Accepted 14th November 2020

DOI: 10.1039/d0ay02014a

rsc.li/methods

This paper presents a method to continuously collect and reliably measure sweat analyte concentrations during exercise. The method can be used to validate newly developed sweat sensors and to obtain insight into intraindividual variations of sweat analytes in athletes. First, a novel design of a sweat collection system is created. The sweat collection patch, that is made from hydrophilized foil and a double-sided acrylate adhesive, consists of a reservoir array that collects samples consecutively in time. During a physiological experiment, sweat can be collected from the back of a participant and the filling speed of the collector is monitored by using a camera. After the experiment, $Na^+$, $Cl^-$ and $K^+$ levels are measured with ion chromatography. Sweat analyte variations are measured during exercise for an hour at three different locations on the back. The $Na^+$ and $Cl^-$ variations show a similar trend and the absolute concentrations vary with the patch location. $Na^+$ and $Cl^-$ concentrations increase and $K^+$ concentrations seem to decrease during this exercise. With this new sweat collection system, sweat $Na^+$, $Cl^-$ and $K^+$ concentrations can be collected over time during exercise at medium to high intensity, to analyse the trend in electrolyte variations per individual.



## Introduction

Recent developments in flexible and wearable electronics for sweat sensing offer new opportunities for gathering physiological information from human beings real-time. Current healthcare systems are moving towards connected care solutions and measuring the physical status of a patient in their home situation. For healthy persons, sweat sensors can potentially play a role in prevention of diseases and to motivate people to exercise. This research focuses on sweat sensing applications in a sports context.

Until now, little is known about how sweat analytes change over time and how they can be used to monitor athletes. The physiological literature about this topic is scattered and papers often show contradicting results. The application of sweat analytes in monitoring the physiological status of athletes is currently limited, because little is known about how sweat analyte concentrations relate to blood values.[1,2]

An important reason for this is the lack of suitable sweat collection methods for physiologists, who are studying the physiological mechanisms behind sweating. Local methods include collection with absorbent patches, pouches and the Macroduct sweat collection system.[3–6] All these methods require repeated placement and removal of these devices when you want to measure electrolyte variations during an exercise. Several challenges of sweat measurement can be identified. Below, the most important challenges are reported, based on the literature and our own experiments.[3,7]

(1) Sweat rates vary over time and influence the sampled ion concentrations.

(2) Due to the low sweat rates per gland (nl $min^{-1}$ $mm^{-2}$), sample volumes are small.

(3) Skin and sweat gland metabolism influence the concentration levels in sweat.

(4) Contamination of new sweat with old sweat or by skin contaminants can occur.

(5) Sample collection is difficult due to evaporation from the highly distributed sweat glands, and the irregular skin surface.

(6) Several sweat analytes, such as glucose and proteins, are present in very low concentrations.

### (A) Electrolytes of interest

This research focuses on measuring electrolytes in sweat to keep track of the physical status of an athlete. Stefaniak and

[a]Delft University of Technology, Faculty of Electrical Engineering, Mathematics & Computer Science, Mekelweg 4, Delft, 2628 CD, The Netherlands. E-mail: a.s.m.steijlen@tudelft.nll

[b]Delft University of Technology, Faculty of Aerospace Engineering, Kluyverweg 1, 2629 HS Delft, The Netherlands

[c]Delft University of Technology, Faculty Industrial Design Engineering, Landbergstraat, 15, Delft, 2628 CE, The Netherlands

† Electronic supplementary information (ESI) available. See DOI: 10.1039/d0ay02014a

Harvey gave an overview of the main constituents in sweat and their median concentrations.[8,9] According to the literature several constituents are of potential interest for monitoring the athlete's physical status during exercise.

Eccrine sweat mainly consists of water and NaCl. $Na^+$ and $Cl^-$ are secreted in the secretory coil of the sweat gland and a part is reabsorbed in the duct. When the sweat rate becomes higher, less ions are reabsorbed in the duct and the concentrations of $Na^+$ and $Cl^-$ are higher.[2,10] Since the concentration varies with the sweat rate, measuring $Na^+$ and $Cl^-$ levels may be useful in determining the sweat rate of an athlete. Several researchers state that $Na^+$ and $Cl^-$ increase when an athlete dehydrates and lower levels of $Na^+$ and $Cl^-$ can indicate electrolyte loss.[1,11] However, papers that present $Na^+$ and $Cl^-$ measurements together with changes in the hydration status, show mixed results.[12] One of the main reasons for this is the lack of standardized collection and analysis methods.

For $K^+$, part of the secretion mechanism is known. However, contradictory results about $K^+$ variations in sweat and the relation of $K^+$ levels to the sweat rate are found in the literature.[13,14] It is also expected that $K^+$ levels are often overestimated due to skin contamination.[15] More research is needed to find out if this parameter turns out to be useful in monitoring the physical status of an athlete.

Although the literature shows contradictory results for $NH_4^+$ measurements as well, some researchers state that $NH_4^+$ levels are related to lactate levels in the blood, which makes this analyte potentially interesting for tracking muscle fatigue.[16–19]

### (B) Technological developments

A large number of newly developed sweat sensors can be found in the recent literature. In the category of electrochemical sensing systems, Guinovart *et al.* created a potentiometric sensor integrated in a tattoo that can measure $NH_4^+$ in sweat.[20] Gao *et al.* designed a sensor array that enables potentiometric measurements of electrolytes, like $Na^+$ and $K^+$ and amperometric measurements of metabolites such as lactate and glucose. Mugo and Alberkant developed a non-enzymatic cortisol sensor that makes use of molecular imprinted polymers for selectivity.[21] In addition, Yuan *et al.* created a sensor that can measure the sweat rate, total ionic charge and sodium concentration.[22] A few examples are presented above. To give an overview of current sweat sensor developments, several literature reviews are published.[23–27]

Secondly, researchers use microfluidics systems for sweat sensing purposes. Ma *et al.* designed a patch that contains a wick and a microfluidic channel that collects the sweat and brings the sweat to the electrode of the sensor.[28] Koh *et al.* created microfluidic channels from PDMS that enabled colorimetric measurement of sweat and Choi *et al.* created a microfluidic network with small bursting valves for chrono-sampling of sweat.[29,30] Sample volumes of the collected sweat in these systems are small (*e.g.* 6 μl). Aranyosi *et al.* created a fluidic system for single but larger samples.[31]

### (C) A new sweat collection system

Although a large number of compact and continuous sweat sensing systems are presented in the recent literature, applications for monitoring an athlete's or patient's status are still limited.

Physiologists lack suitable collection and analysis systems for continuous monitoring to find useful sweat biomarkers and how they change over time. In the technological literature, validation of novel sweat sensor systems in human trials appears difficult, because there are no standardized methods to perform reference measurements by chrono sampling sweat and analysing it in the lab afterwards. To solve these problems, we propose a new sweat collection device that can automatically collect a sequence of sweat samples (>100 μl). The system is easier to fabricate and the collection surface is larger than in previously presented solutions, which facilitates the use of the system by both engineers and physiologists and increases reliability of the measurements. Physiological experiments and chromatography measurements are executed to prove that this method can be used to analyse electrolyte variations over time.

The sweat collector device can in principle be connected to an electrochemical sensing system for continuous measurements. The testing of our new sweat collectors with an *in situ* analysis system will be discussed in a subsequent paper.

## Method

In order to allow for continuous uptake of sweat volumes and to simplify the collector placement step, it was decided to develop a simple disposable foil type sensor patch that can automatically collect a sequence of 5 samples. The design, simulations of the inflow of sweat and lab experiments are presented first. After demonstrating the working principle of the collector, the new system is tested in a physiological experiment. Sweat is collected with the new patch during exercise and analysed in the lab with ion chromatography. This is presented in Section (B–D).

### (A) Design & simulations

The fluidic system contains a sequence of reservoirs that are created from two layers of hydrophilic film (Visgard 275,[32] a PET film with a PU coating) with a double-sided adhesive (3M 1522,[33] a PE tape with an acrylate adhesive) in between.

**(1) Design.** In Fig. 1, an exploded view and a front view of the final design of the sweat collection system are presented. The sweat collection surface is 40 $cm^2$. The funnel-shaped 2D structure of the skin adhesive (Fig. 1, no. 1) guides the sweat to the inlet. In combination with the grating structure, it serves as a spacer to the skin too, to make sure that the sweat drops down.

Due to capillary forces, the sweat flows from the inlet (Fig. 1, no. 7.) to the reservoirs (Fig. 1, no. 10.). The walls of the capillaries are highly hydrophilic to ensure that the flow rate of sweat is not negatively influenced by the channels. The sweat passes a T-junction (Fig. 1, no. 8) at a certain moment. At this junction the sweat needs to flow down into the reservoir. By creating

 

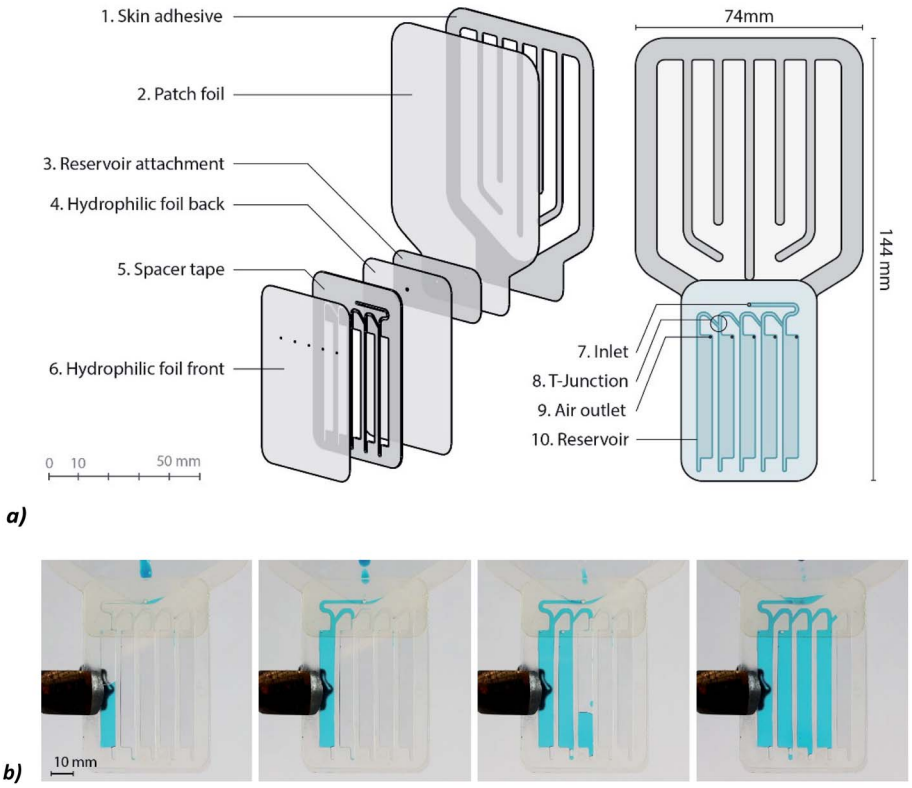


Fig. 1 Design of the sweat patch: (a) left: exploded view, right: front view of the patch. (b) The filling process of the reservoirs.

sharp edges at the junction and by directing the left branch of the junction upwards, it is ensured that the sweat goes straight into the reservoir. When the reservoir is filled, the sweat will take the left turn and will flow to the next reservoir by capillary forces. Entrapment of air is prevented by placing air outlets (Fig. 1, no. 9) at the right corner of each reservoir.

The materials were cut into the desired shapes with a $CO_2$ laser system (Merlin Lasers, Lion Laser Systems, The Netherlands). The film is rinsed with demineralized water (to remove the extra ionic surfactant that was applied to the film by the manufacturer, because it influenced the sodium measurements in preliminary experiments). Samples of the foil and adhesive were placed in vials with demineralized water (3 ml, 24 hours), and ion concentrations ($Na^+$, $Cl^-$ and $K^+$) in these vials were analysed to ensure the absence of background contaminants from the materials. No significant $Na^+$, $Cl^-$ and $K^+$ peaks were detected in these samples. Contact angles of the materials were measured with optical tensiometry (KSV Instruments Ltd). The spacer tape has an average contact angle of 50.5° and the hydrophilic foil has an average contact angle of 92.2° (Fig. S1, ESI†).

**(2) Simulations.** Gravitation and capillary effects are used to make sure that the sweat flows into the reservoirs at a similar or faster volumetric flow rate than the sweat rate. The capillary effects depend on the surface tension and the geometry of the tube. A relation between the capillary pressure and the contact angle and dimensions of the microchannel with a certain height ($h$) and width ($w$) is given by the Young–Laplace equation:

$$P = -\gamma\left[\frac{\cos\theta_t + \cos\theta_b}{h} + \frac{\cos\theta_l + \cos\theta_r}{w}\right] \quad (1)$$

where $P$ is the capillary pressure, $\gamma$ the surface tension of the liquid and $\theta_t$, $\theta_b$, $\theta_l$, and $\theta_r$ are the contact angles of the top, bottom, left and right microchannel walls. For the design of capillary channels, there are a few practical guidelines. First, contact angles smaller than 60° are preferred.[34] Secondly, some of the walls of a microchannel can be made of a hydrophobic material if one takes into account that the ratio between, for example, the hydrophobic height and the hydrophilic width of the channel is very low. Furthermore, fluid flow near corners needs to be considered since it can affect the filling of the channels negatively by entrapment of air bubbles.[35] It can be prevented by rounding the edges and corners of the channels, for example.

Several designs were made and CFD simulations with COMSOL Multiphysics software were performed to test the functioning of the devices. For the simulations it is assumed that water can flow freely into the channel (ideal case). The transport of the fluid interface is given by a level set function.[36]

This function is coupled with the Navier–Stokes equations to describe mass and momentum transport of the fluid. The velocity of the fluid is dependent on convection, pressure, diffusion, the surface tension and gravity in this model.

Initially, a small reservoir at the beginning of the microchannels is filled with water and the rest of the channels and the big reservoir are filled with air. The initial velocity is 0. A

hydrostatic pressure is applied at the inlet of the channels ($P = \rho \times g \times y$) and the pressure at the outlet is 0. Atmospheric pressure can be omitted since it is acting on both the inlet and the outlet. The gravity is added to the model as a volume force. The wetted wall feature is used to identify hydrophobic and hydrophilic walls.

First, the influences of the spacer tape and corner flow effects were simulated with a straight channel. Second, parts of the collection patch were simulated to test if the reservoirs are filled in the right way and to prevent entrapment of air.

### (B) Syringe pump experiments

A syringe pump experiment is executed to test if the reservoirs will be filled one after the other and to research if the sweat flow in the collector is the same as the actual sweat rate.

The syringe pump (KDScientific 200, USA) is set at a rate of 48 μl $min^{-1}$. Via the funnel-shaped structure, the sweat will drop down towards the inlet of the reservoirs.

The collector is designed to be placed on the back of an athlete. The back is chosen, because of the high sweat rate and the presence of eccrine sweat glands at this location. Smith and Havenith measured a sweat rate at the back of 1.2 mg $cm^{-2}$ $min^{-1}$ during a running exercise at around 155 bpm of 30 min (25.6 ± 0.4 °C, 43.4 ± 7.6% relative humidity).[37] The patch will have a collection surface of 40 $cm^2$, which means that the sweat rate will be around 48 μl $min^{-1}$.

Collector filling is recorded with a camera. After the experiment, stills are taken from the movie. Due to the blue colorant that was added to the fluid, all blue pixels in the image can be counted to derive the volume that was filled with fluid. This process was automated with a MATLAB program.

### (C) Physiological experiments

The physiological experiments were approved by the Human Research Ethics Committee of Delft University of Technology. The participants gave informed consent before the experiment. Healthy recreational athletes ($n$ = 5, 20–30 years) that play sports 2 to 5 times a week were asked to cycle for one hour on a cycle ergometer. The ergometer is equipped with a cadence meter, power meter (Garmin Vector 3s) and cycling computer, a Garmin Edge 820 (Garmin, USA), that is placed at the handlebar (Fig. 2a). The subject wears a heart rate monitor and sweat collectors are placed at the back. A camera is placed behind the cyclist and focused on the sweat collectors to measure the filling speed. After placement of the heart rate belt and the first sweat patches, the subject is asked to cycle for one hour at a constant cadence and power output (in the final experiment a cadence of: $M$ = 91, STD = 5 rpm, heart rate: $M$ = 158, STD = 11 bpm and power: $M$ = 284, STD = 28 W were measured (Fig. S2, ESI†), the temperature of the room was 20 °C). Two preliminary tests were performed before the final experiment to improve the test setup. Preliminary results (Fig. S3, ESI†) show the importance of a strict and optimized test protocol. In the final experiment, the skin was cleaned with a sterile gauze pad that was wetted with demineralized water. This was executed two times before each patch was placed to avoid accumulation of old sweat constituents.

In the first two series of experiments the collectors were replaced at the same location, when a collector was filled completely. Unfortunately, a replaced collector does not start filling immediately (it can take approximately 10 minutes). To improve the continuity of the sweat measurements, the patches were placed as shown in Fig. 2b in the final experiment. Patch B can now be placed 10 minutes before patch A is filled and more sweat can be collected. It is assumed that the sweat rates at locations left and right of the spine are identical.

### (D) Chemical analysis

After sweat collection, transfer to vials is done by perforating the bottom tip of the reservoir on one side. A syringe with air is placed at the air inlet of the reservoir and the sweat is forced out through the perforated tip to the vial. Before each perforation of a reservoir, the outside of the collector is cleaned to prevent one sample contaminating the other (Fig. S4, ESI†). Approximately

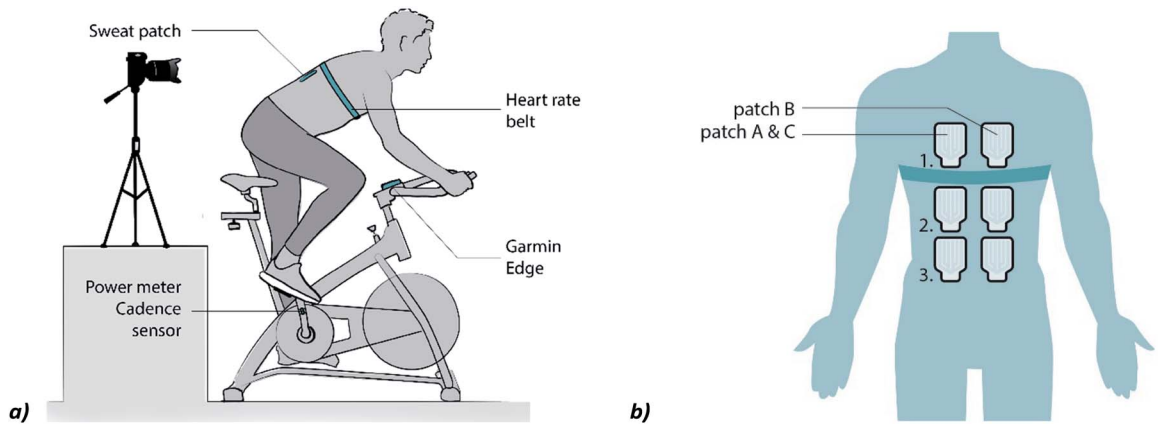


Fig. 2 (a) Setup of the physiological experiment (reproduced from ref. 38). (b) Placement of the patches in the final experiment. The patches A (location 1, 2 and 3) are placed at the start. Patches B (1, 2 and 3) are placed when patches A start filling. Patches of C (1–3) are placed when A is filled.

 

5% of the sweat in each reservoir is lost during transfer. The sweat is diluted with 3 ml of ultra-pure water. The samples are stored in a fridge at 7 °C. The day after, the sweat is analysed using ion chromatography/high pressure liquid chromatography (IC/HPLC)[39] The IC system consists of a Metrohm 881 Anion system and an 883 Basic IC plus system (Metrohm, Switzerland). The two systems work independently. Both devices contain an HPLC pump that pumps the eluent through a column that separates the ions. After separation, the conductivity of the fluid is measured by the conductivity detector.

To analyse the cations, a Metrosep C6 – 150/4.0 column is used for separation with a solution of 3 mM $HNO_3$ as the eluent. The flow rate is set at 0.9 ml $min^{-1}$. For the anions, a Metrosep A supp 5 – 150/4.0 column is used, and chemical suppression is performed by using the Metrohm Suppressor Module, which is regenerated with 150 mM $H_3PO_4$. The eluent of the anion system contains 1 mM $NaHCO_3$ and 3.2 mM $Na_2CO_3$. The flow rate in this system is 0.7 ml $min^{-1}$. A sample loop of 20 μl is used in both systems.

Before each analysis, standards need to be made for all the ions of interest. Solutions with 0.1 till 100 ppm are made. The measurements of the standards are used for calibration. After assigning manually the right retention times to the peaks, the MagIC Net software, automatically creates a calibration graph based on the peak areas which can be applied to the measurements.

To quantify the accuracy of our method, standard deviation experiments are executed. Standard solutions with 0.1 to 100 ppm $Na^+$, $NH_4^+$ and $K^+$ ions and separate solutions with $Cl^-$ ions are prepared. The solutions are divided into 5 samples and measured one by one to obtain an idea of the standard deviation of the method at different concentration levels.

## Results & discussion

The results of the simulations and lab experiments are presented first. Thereafter, the results from the physiological experiments are discussed.

### (A) Design & simulations

A first simulation was executed to find out the effect of the hydrophobicity of a spacer tape (sidewalls of the channels) on the volumetric flow rate in the channels. The dimensions of the simulated channel are 2 × 0.25 × 4 mm. Contact angles of $\theta = 112.5°$ and $\theta = 67.5°$ are chosen for the hydrophobic walls and the hydrophilic sidewalls, respectively.

To study the effect of corner flow, channels with rounded corners and the same dimensions as the previous channel are simulated as well. One channel has hydrophobic rounded sidewalls and the other has hydrophilic rounded sidewalls. Fig. 3a shows the influence of the rounded and sharp, hydrophilic, and hydrophobic sidewalls on the contact point position of the fluid–air interface over time. The volumetric flow rate decreases significantly when the hydrophobic sidewalls have rounded corners. Since the laser cut spacer tape is placed on top of another layer of foil, the corners will be relatively sharp.

Simulations are also performed to test whether the T-junction works suitably. In Fig. 3b it can be seen that the fluid first flows down and once the water reaches the bottom ($t = 5$ ms), it goes left to the next reservoir.

Lastly, a simulation was performed to check if entrapment of air would be a problem in the reservoirs. Fig. 3c shows that the fluid does not block the air outlet during the filling process, so that air bubbles can be released. The filling time of a reservoir with a height of 10 mm, is now very small. This is due to the infinite supply of water at the inlet. The sweat rate will limit the fluid supply in reality. However, the simulation shows that even with an infinite supply of water, the reservoir is filled in the right way. This accounts for the T-junction as well.

### (B) Syringe pump experiments

Fig. 1 shows stills from one of the movies that is made during the syringe pump experiments, which prove that the reservoirs are filled consecutively. The measurement results of the experiment are shown in Fig. 3d. A delay of 50 to 80 seconds is observed before the fluid is in the reservoirs and recorded by using a camera. The average volumetric flow rate in the collector is 47 μl $min^{-1}$, which means that the flow rate in the collector is 2% lower. From this we can conclude that the fluid inflow is not significantly inhibited by the resistance of the channels.

### (C) Physiological experiments & chemical analysis

After sweat collection during the physiological experiments, the sweat in the collectors is analysed using ion chromatography/high pressure liquid chromatography (IC/HPLC). In the chromatographs of our sweat samples, the peaks are nicely separated and there are no significant unknown peaks that interfere with the peaks of the selected ions (Fig. S5, ESI†).

To get an idea of the standard deviation that is introduced by the IC measurement method, standard deviations of the method are included. These are determined by analysing five samples of each standard (0.1–100 ppm) and plotting the average relative standard deviations (RSDs) in a graph (Fig. 4a). The fitting curve is used to determine the SDs in the actual measurements. For $Cl^-$ and $Na^+$ the SDs are relatively small, for $K^+$, the concentrations in sweat are around ten times lower so the RSDs of the measurement method become important to consider. The measured concentration levels of $Na^+$, $Cl^-$ and $K^+$ of patch location 2 are shown in Fig. 4b. The $Na^+$ and $Cl^-$ concentrations show an initial steady increase which levels off. However, $Cl^-$ levels are systematically lower by an average of 16.4 mM (SD = 2.5 mM) than the $Na^+$ levels. This deviation can possibly be explained by the presence of other negative ions like lactate and bicarbonate ($C_3H_5O_3^-$ and $HCO_3^-$) in sweat.

In Fig. 4c, the $Na^+$, $Cl^-$ and $K^+$ levels of patch location 1 (between the shoulder blades) and 3 (lower back) are added. The $Na^+$ and $Cl^-$ levels are very similar for collector 2 and 3 ($Cl^-$: $M$ (mean) = 1.6, SD= 2.9, $Na^+$: $M = 0.4$, SD = 3.4 mM) while the $Na^+$ and $Cl^-$ levels of collector location 1 are significantly higher

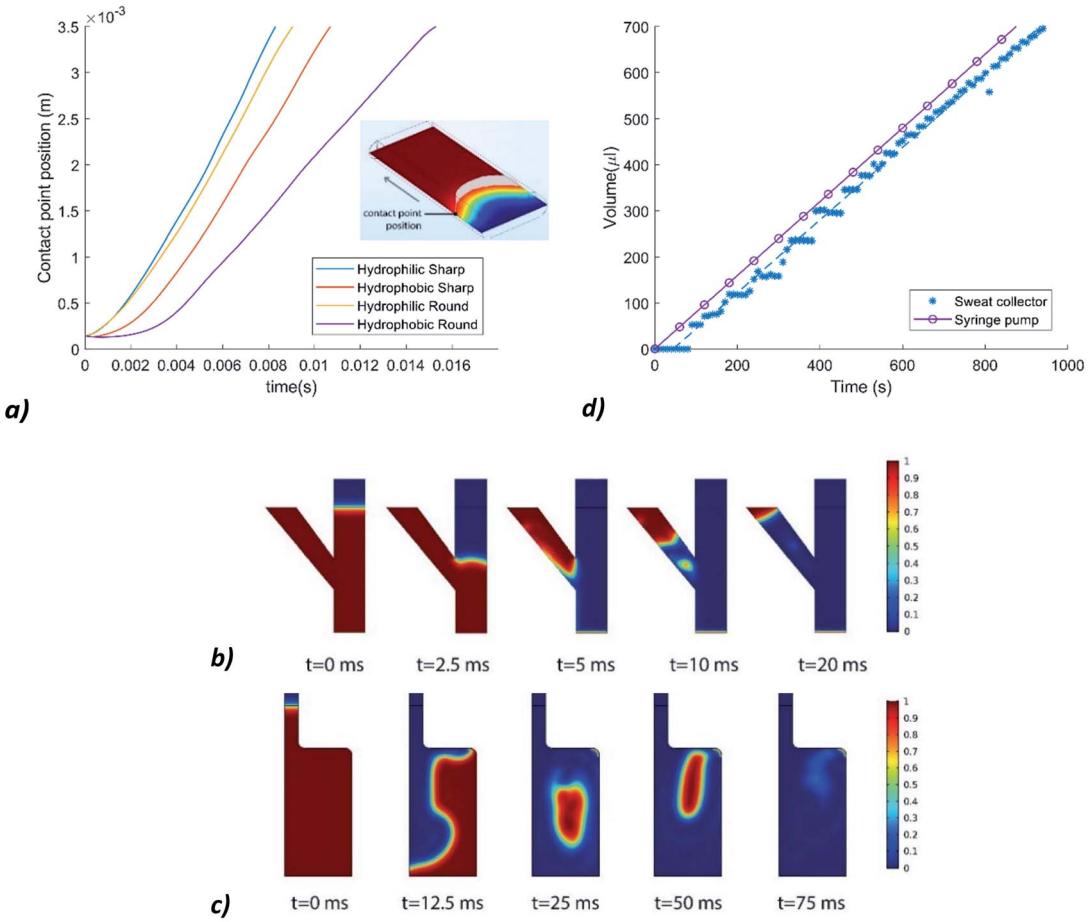


Fig. 3 (a) Contact point position of the fluid–air interface over time of designs with rounded and sharp, hydrophilic and hydrophobic sidewalls. (b) Simulation of the T-junction: volume fraction of air at different time points. (c) Simulation of the reservoir: volume fraction of air at different time points. (d) Volumetric flow rate of the syringe pump *vs.* the volumetric flow rate in the collector.

($Cl^-$: $M = 10.3$, SD $= 2.4$, $Na^+$: $M = 10.4$, SD $= 2.9$ mM). One of the reasons for this difference between the absolute concentrations of collector 1 and collector 2 and 3 is the variation in the sweat rate across the different locations. Smith and Havenith measured at the sides of the upper back a median sweat rate of 0.84 mg $cm^{-2}$ $min^{-1}$, while at the sides of the lower back this sweat rate was 0.75 mg $cm^{-2}$ $min^{-1}$.[37] Higher sweat rates decrease ion reabsorption per unit volume and therefore higher concentrations can be measured at the upper back.

Fig. 4d shows the $K^+$ levels at the three locations over time. A decrease is measured over time and no difference between the three locations can be detected within the error margin. To test whether the trend is still a decreasing line, when taking the large SDs into account, random samples and their linear fits ($n = 1000$) were created, assuming a normal distribution.

Within the 95% confidence interval, the fits for location 1 and 2 were always a decreasing line. However, from the literature it was assumed that only minimal changes in $K^+$ levels occur in sweat.[9] Therefore, it is expected that elevated values after the start of the exercise are due to the presence of old sweat or residue in the channels or other physiological effects that need further research.

Because an increased sweat rate leads to less ion reabsorption in the reabsorptive duct, sweat rate measurements are important as well. The sweat collection rate is measured at location 2 during the experiments with the help of a camera. The average sweat rate is 1.19 mg $cm^{-2}$ $min^{-1}$. The sweat collection rate varied between 0.74 and 1.54 mg $cm^{-2}$ $min^{-1}$ (Fig. 5a).

The sweat rate was plotted against the concentration of $Na^+$ and $Cl^-$, to check whether this relation was visible. The data allows us in principle to verify a possible relation between the sweat rate and $Na^+$ and $Cl^-$ concentrations. Although the plot of Fig. 5b suggests a mild increase in ion concentrations with increasing sweat rate, the scatter in the current data is too large to draw a solid conclusion. In a next phase of this project, other sweat rate measurement techniques will be explored by, for example, conductive or capacitive measurements. It would also be interesting to compare this new method of sweat rate measurement with conventional methods like the ventilated capsule measurement and the absorbent patch method in the same physiological experiment.[40]

 

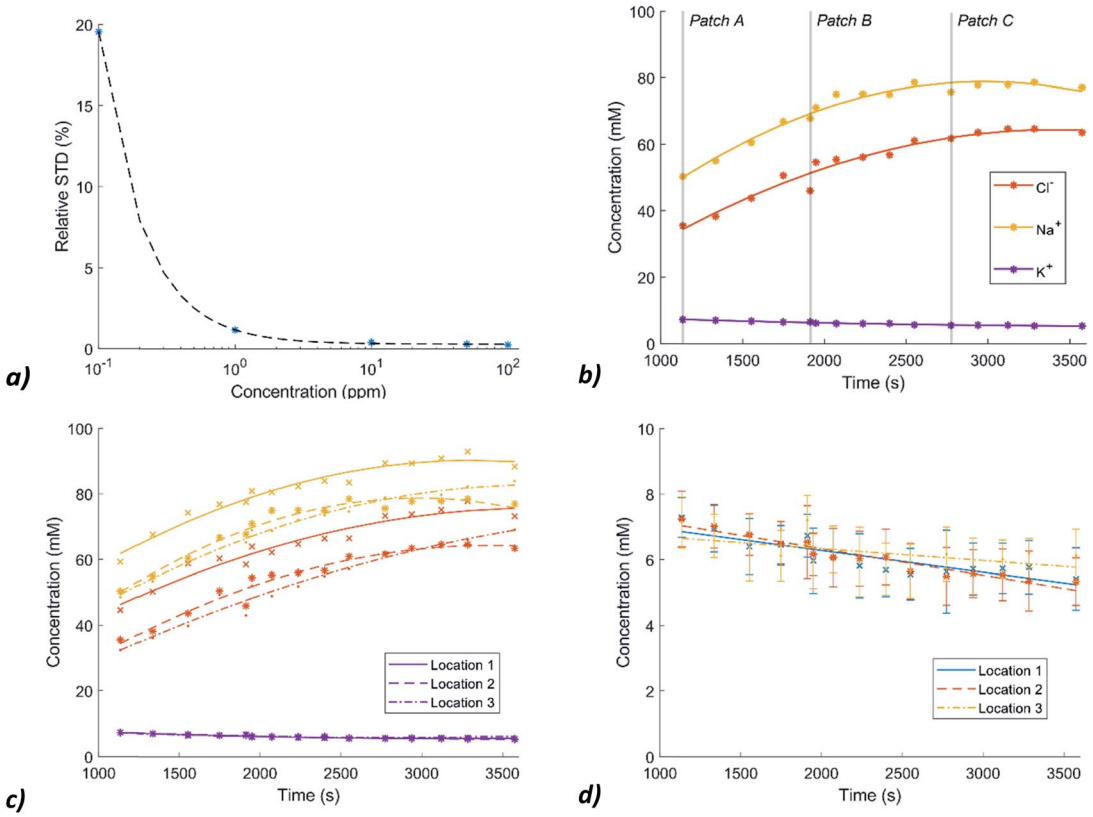


Fig. 4 (a) The accuracy of the IC method: relative standard deviation at different ion concentration levels of standard solutions. (b) the $Na^+$ (top), $Cl^-$ (middle) and $K^+$ (bottom) levels of patch location 2. (c) the $Na^+$ (top), $Cl^-$ (middle) and $K^+$ (bottom) levels of patch locations 1,2 and 3. (d) $K^+$ concentrations over time for patch locations 1,2 and 3.

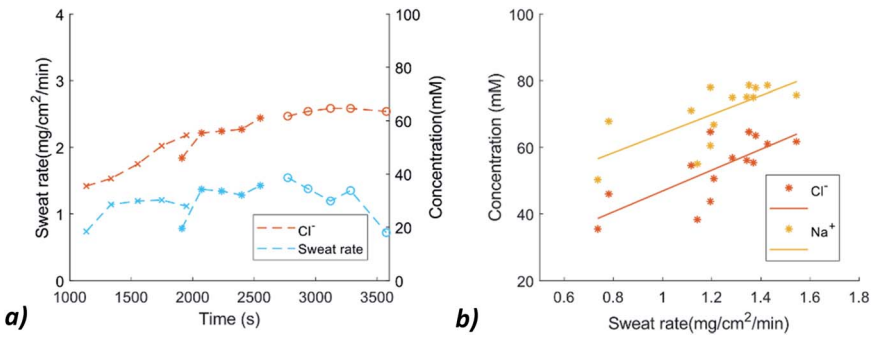


Fig. 5 (a) Sweat rate and $Cl^-$ variation over time (b) Relation between the sweat rate and $Na^+$ and $Cl^-$ concentration.

## Conclusion

The results of the final physiological experiment show that $Na^+$, $Cl^-$ and $K^+$ can be measured accurately with this new collection system in combination with ion chromatography. Although the $Na^+$ and $Cl^-$ concentrations differ when the collector is placed at the upper back, all three collector locations show a similar trend in $Na^+$ and $Cl^-$ levels. $K^+$ measurements are also reproducible, and a decreasing trend is measured.

In the current study, data from only one physiological experiment of a single individual are compared, because it is well known that sweat analyte concentrations can differ considerably between individuals and that the day-to-day variability in sweat analyte concentrations can be large. Therefore, comparing, and interpreting data between individuals in small scale experiments would be less relevant.

However, the presently developed device will facilitate more systematic larger studies on the inter-individual variability as well as the daily variations of sweat electrolytes in a single individual. In this way, the new device can contribute to a better understanding of sweat mechanisms and their relation to blood values, to find useful biomarkers in sweat to monitor the status of an athlete.

## Conflicts of interest

There are no conflicts to declare.

## Acknowledgements

The authors thank Armand Middeldorp for his support in ion chromatography and X TU Delft for sharing their sports facilities. This work is part of the research program Citius, Altius, and Sanius with project number P16-28, which is financed by the Dutch Research Council (NWO).

## References

1 Z. Sonner, E. Wilder, J. Heikenfeld, G. Kasting, F. Beyette, D. Swaile, F. Sherman, J. Joyce, J. Hagen, N. Kelley-Loughnane and R. Naik, *Biomicrofluidics*, 2015, **9**, 031301.
2 L. B. Baker, *Temperature*, 2019, **6**, 211–259.
3 L. B. Baker, *Sports Medicine*, 2017, **47**, 111–128.
4 B. A. Katchman, M. Zhu, J. Blain Christen and K. S. Anderson, *PROTEOMICS – Clinical Applications*, 2018, **12**, 1800010.
5 L. Klous, C. De Ruiter, P. Alkemade, H. Daanen and N. Gerrett, *Journal of Thermal Biology*, 2020, **93**, 102697.
6 K. Hooton and L. Li, *Analytical Chemistry*, 2017, **89**, 7847–7851.
7 J. Heikenfeld, *Electroanalysis*, 2016, **28**, 1242–1249.
8 A. B. Stefaniak and C. J. Harvey, *Toxicology in Vitro*, 2006, **20**, 1265–1283.
9 C. J. Harvey, R. F. LeBouf and A. B. Stefaniak, *Toxicology in Vitro*, 2010, **24**, 1790–1796.
10 K. Sato, W. H. Kang, K. Saga and K. T. Sato, *J Am Acad Dermatol*, 1989, **20**, 537–563.
11 R. M. Morgan, M. J. Patterson and M. A. Nimmo, *Acta Physiol Scand*, 2004, **182**, 37–43.
12 L. B. Baker and A. S. Wolfe, *Eur J Appl Physiol*, 2020, **120**, 719–752.
13 B. G. Holmes N, Y. Zhao, J. Sherriff and V. Miller, *Ann Sports Med Res*, 2016, **3(2)**(1, 2), 1063.
14 M. J. Patterson, S. D. Galloway and M. A. Nimmo, *Experimental physiology*, 2000, **85**, 869–875.
15 M. R. Ely, R. W. Kenefick, S. N. Cheuvront, T. D. Chinevere, C. P. Lacher, H. C. Lukaski and S. J. Montain, *J. Appl. Physiol.*, 2011, **110**, 1534–1540.
16 W. Ament, J. R. Huizenga, G. A. Mook, C. H. Gips and G. J. Verkerke, *Int J Sports Med*, 1997, **18**, 35–39.
17 I. Alvear-Ordenes, D. Garcia-Lopez, J. A. De Paz and J. Gonzalez-Gallego, *Int J Sports Med*, 2005, **26**, 632–637.
18 A. Zoerner, S. Oertel, M. P. M. Jank, L. Frey, B. Langenstein and T. Bertsch, *Electroanalysis*, 2018, **30**, 665–671.
19 N. V. Bhagavan and C.-E. Ha, in *Essentials of Medical Biochemistry*, 2011, pp. 241–259, DOI: 10.1016/b978-0-12-095461-2.00019-9.
20 T. Guinovart, A. J. Bandodkar, J. R. Windmiller, F. J. Andrade and J. Wang, *Analyst*, 2013, **138**, 7031–7038.
21 S. M. Mugo and J. Alberkant, *Analytical and Bioanalytical Chemistry*, 2020, **412**, 1825–1833.
22 Z. Yuan, L. Hou, M. Bariya, H. Y. Y. Nyein, L.-C. Tai, W. Ji, L. Li and A. Javey, *Lab on a Chip*, 2019, **19**, 3179–3189.
23 T. Kaya, G. Liu, J. Ho, K. Yelamarthi, K. Miller, J. Edwards and A. Stannard, *Electroanalysis*, 2019, **31**, 411–421.
24 M. Bariya, H. Y. Y. Nyein and A. Javey, *Nature Electronics*, 2018, **1**, 160.
25 M. Parrilla, M. Cuartero and G. A. Crespo, *TrAC Trends in Analytical Chemistry*, 2019, **110**, 303–320.
26 J. Choi, R. Ghaffari, L. B. Baker and J. A. Rogers, *Science advances*, 2018, **4**, eaar3921.
27 M. Chung, G. Fortunato and N. Radacsi, *Journal of The Royal Society Interface*, 2019, **16**, 20190217.
28 B. Ma, J. Chi, C. Xu, Y. Ni, C. Zhao and H. Liu, *Talanta*, 2020, 120786, DOI: 10.1016/j.talanta.2020.120786.
29 A. Koh, D. Kang, Y. Xue, S. Lee, R. M. Pielak, J. Kim, T. Hwang, S. Min, A. Banks, P. Bastien, M. C. Manco, L. Wang, K. R. Ammann, K.-I. Jang, P. Won, S. Han, R. Ghaffari, U. Paik, M. J. Slepian, G. Balooch, Y. Huang and J. A. Rogers, *Science Translational Medicine*, 2016, **8**, 366ra165.
30 J. Choi, D. Kang, S. Han, S. B. Kim and J. A. Rogers, *Adv Healthc Mater*, 2017, **6**(5), 1601355.
31 A. J. Aranyosi, J. B. Model, M. Z. Zhang, S. P. Lee, A. Leech, W. Li, M. S. Seib, S. Chen, N. Reny, J. Wallace, M. H. Shin, A. J. Bandodkar, J. Choi, A. S. Paller, J. A. Rogers, S. Xu and R. Ghaffari, *Journal of Investigative Dermatology*, 2020, DOI: 10.1016/j.jid.2020.05.107.
32 R. G. La Casse and W. S. Creasy, *US pat.*, 5877254A, 1999.
33 *3M, Technical Information Sheet Product Number #1522 3MTM Double Coated Medical Tape*, https://multimedia.3m.com/mws/media/792049O/3m-1522-dc-polyethylene-tape-tis-jul13.pdf, accessed 06 December 2019.
34 J. Berthier, in *Micro-Drops and Digital Microfluidics*, ed. J. Berthier, William Andrew Publishing, 2nd edn, 2013, pp. 7–73, DOI: 10.1016/B978-1-4557-2550-2.00002-X.
35 Z. Wu, Y. Huang, X. Chen and X. Zhang, *International Journal of Multiphase Flow*, 2018, **109**, 14–25.
36 Comsol Inc, *Capillary Filling - Level Set Method*, https://www.comsol.com/model/capillary-filling-8212-phase-field-method-1878, accessed at 26 Novermber 2020.
37 C. J. Smith and G. Havenith, *European Journal of Applied Physiology*, 2011, **111**, 1391–1404.
38 A. S. M. Steijlen, J. Bastemeijer, W. A. Groen, K. M. B. Jansen, P. J. French and A. Bossche, *IEEE Engineering in Medicine & Biology Society (EMBC) Proc.*, 2020, pp. 4085–4088, DOI: 10.1109/EMBC44109.2020.9176123.
39 J. Doorn, T. Storteboom, A. Mulder, W. de Jong, B. Rottier and I. Kema, *Annals of clinical biochemistry*, 2015, **52**, 421–427.
40 N. B. Morris, M. N. Cramer, S. G. Hodder, G. Havenith and O. Jay, *Journal of applied physiology*, 2013, **114**, 816–823.

 